Limnol. Oceanogr., 58(3), 2013, 997–1007

doi:10.4319/lo.2013.58.3.0997

Sensitivity of Antarctic phytoplankton species to ocean acidification: Growth, carbon acquisition, and species interaction

Scarlett Trimborn,* Tina Brenneis, Elizabeth Sweet, and Björn Rost

Alfred Wegener Institute for Polar and Marine Research, Bremerhaven, Germany

Abstract

Despite the fact that ocean acidification is considered to be especially pronounced in the Southern Ocean, little is known about CO_2-dependent physiological processes and the interactions of Antarctic phytoplankton key species. We therefore studied the effects of CO_2 partial pressure (P_{CO_2}) (16.2, 39.5, and 101.3 Pa) on growth and photosynthetic carbon acquisition in the bloom-forming species *Chaetoceros debilis, Pseudo-nitzschia subcurvata, Fragilariopsis kerguelensis,* and *Phaeocystis antarctica.* Using membrane-inlet mass spectrometry, photosynthetic O_2 evolution and inorganic carbon (C_i) fluxes were determined as a function of CO_2 concentration. Only the growth of *C. debilis* was enhanced under high P_{CO_2}. Analysis of the carbon concentrating mechanism (CCM) revealed the operation of very efficient CCMs (i.e., high C_i affinities) in all species, but there were species-specific differences in CO_2-dependent regulation of individual CCM components (i.e., CO_2 and HCO_3^- uptake kinetics, carbonic anhydrase activities). Gross CO_2 uptake rates appear to increase with the cell surface area to volume ratios. Species competition experiments with *C. debilis* and *P. subcurvata* under different P_{CO_2} levels confirmed the CO_2-stimulated growth of *C. debilis* observed in monospecific incubations, also in the presence of *P. subcurvata*. Independent of P_{CO_2}, high initial cell abundances of *P. subcurvata* led to reduced growth rates of *C. debilis*. For a better understanding of future changes in phytoplankton communities, CO_2-sensitive physiological processes need to be identified, but also species interactions must be taken into account because their interplay determines the success of a species.

The Southern Ocean (SO) is a high-nutrient low-chlorophyll region. Compared with most other regions of the World oceans, the concentrations of nitrate and phosphate are high. The reason for this phenomenon is that the biological production is limited by the trace metal iron, which is essential for photosynthesis (Martin et al. 1990). Most of the primary production in the SO is achieved by sporadic bloom events, which mainly occur along the continental margins and only extend offshore when iron and other nutrient concentrations are high due to upwelling. These blooms are usually dominated by medium-sized diatoms and the flagellate *Phaeocystis antarctica* (Smetacek et al. 2004). Light is also a major factor controlling phytoplankton growth and productivity in the SO due to the occurrence of strong and frequent winds, causing pronounced deep mixing and therefore low mean and highly varying light levels (Tilzer et al. 1985). Deeply mixed layers were associated with a predominant occurrence of *P. antarctica,* while diatoms such *Fragilariopsis cylindrus* seem to favor shallow mixed layers (Kropuenske et al. 2010).

Varying CO_2 concentrations were found to also influence SO phytoplankton assemblages and growth (Tortell et al. 2008*b;* Feng et al. 2010). During winter time, the presence of sea ice prevents gas exchange between surface water and the atmosphere, causing CO_2 partial pressure (P_{CO_2}) to often exceed atmospheric levels after ice-out in spring. With increasing light availability, phytoplankton growth causes CO_2 to decrease. Intense photosynthetic activity can result in P_{CO_2} values < 20 Pa toward the end of bloom periods (Arrigo et al. 1999; Cassar et al. 2004). Next to these productivity-related changes in seawater carbonate chemistry, the rise in atmospheric CO_2 levels due to human-induced activities such as fossil fuel burning can have a pronounced effect on phytoplankton growth. At present-day, atmospheric CO_2 concentrations are ~39 Pa, leading to a seawater pH of ~ 8.1. By the end of this century, the ongoing CO_2 emissions are expected to cause atmospheric CO_2 to rise up to 75 Pa and to lower seawater pH to ~ 7.9 ('ocean acidification'; Houghton et al. 2001). As a greenhouse gas, the rise in atmospheric CO_2 will also cause global temperatures to increase, an effect being particularly pronounced in polar regions (Sarmiento et al. 2004). Both the disproportional strong warming and the freshwater input from sea ice melting contribute to enhanced surface stratification in the SO, which in turn may alter the mixing and light regime experienced by phytoplankton. All these environmental changes (CO_2, temperature, light) will affect SO phytoplankton in many, and most likely different, ways.

In order to understand how SO phytoplankton will respond to climate change, knowledge on the physiology and ecology of Antarctic key phytoplankton species is required. The mode of carbon acquisition determines, to a large extent, how phytoplankton respond to changes in CO_2. The CO_2 sensitivity in photosynthesis is mainly the result of the poor affinity of the enzyme Ribulose-1,5-bisphosphate carboxylase/oxygenase (RubisCO) for its substrate CO_2. To overcome potential carbon limitation under present-day CO_2 concentrations, marine phytoplankton operate carbon concentrating mechanisms (CCMs) that enrich CO_2 at the catalytic site of RubisCO and thus enhance their photosynthetic productivity (Giordano et al. 2005). Antarctic natural phytoplankton communities were found to operate constitutive CCMs over a range of various

* Corresponding author: scarlett.trimborn@awi.de

Table 1. P_{CO_2}, CO_2, and dissolved inorganic carbon (DIC) were calculated from total alkalinity (TA), pH, silicate, phosphate, temperature, and salinity using the CO2Sys program (Pierrot et al. 2006).

Target P_{CO_2} (Pa)	P_{CO_2} (Pa)	CO_2 (μmol kg^{-1})	DIC (μmol kg^{-1})	TA (μmol kg^{-1})	pH (NBS)
High, 101.3	98±7	51±5	2247±38	2308±32	7.77±0.03
Ambient, 39.5	39.3±1.3	24±2	2067±34	2244±42	8.12±0.02
Low, 16.2	16.1±0.8	9±0.5	1978±23	2294±15	8.47±0.02

CO_2 concentrations (Cassar et al. 2004; Tortell et al. 2010; Neven et al. 2011). In monocultures of the sea-ice diatom *Nitzschia*, Mitchell and Beardall (1996) revealed CCM activity, but its efficiency and regulation with respect to changes in P_{CO_2} remains unclear. Using the Antarctic diatom *Chaetoceros brevis,* Boelen et al. (2011) investigated the effect of CO_2 under different dynamic light scenarios, focusing on photophysiological responses rather than carbon acquisition. In conclusion, while there is increasing information on Antarctic natural phytoplankton communities, laboratory studies on the physiological characterization of CCMs in Antarctic phytoplankton key species are still scarce.

Next to the CO_2-sensitivity of a species, the knowledge about the interaction between species also is of importance for a better understanding of how SO phytoplankton will respond to ocean acidification. To date, it has not been tested whether a species that benefits from elevated P_{CO_2} in monospecific incubations will also translate this into a competitive advantage over another competitor. Especially toward the end of blooms, when the photosynthetic carbon drawdown exceeds the re-equilibration with the atmosphere, pH and CO_2 effects have been shown to influence species competition (Hansen 2002).

The CO_2 sensitivity in growth and photosynthetic carbon acquisition was studied in four SO phytoplankton species that are relevant in both ecological as well as biogeochemical terms. We grew *Chaetoceros debilis*, *Pseudo-nitzschia subcurvata*, *Fragilariopsis kerguelensis,* and *Phaeocystis antarctica* in monocultures under glacial, present-day, and future P_{CO_2} levels. Using membrane-inlet mass spectrometry (MIMS), photosynthetic O_2 evolution and inorganic carbon (C_i) fluxes were determined as a function of CO_2 concentrations. To further characterize the CCM of each species, measurements of extracellular carbonic anhydrase (CA) activities were performed by monitoring ^{18}O exchange from doubly labeled $^{13}C^{18}O_2$. To test for species interactions, competition experiments were carried out with *C. debilis* and *P. subcurvata* in mixed cultures simulating different bloom and CO_2 scenarios.

Methods

Culture conditions—The diatoms *Chaetoceros debilis* (R/V *Polarstern* cruise ANT-XXI/3, European iron fertilization experiment [EIFEX], In-Patch, 2004, 49°36S, 02°05E, isolated by Philipp Assmy), *Pseudo-nitzschia subcurvata* (R/V *Polarstern* cruise ANT-XXI/4 in Apr 2004 at 49°S, 02°E, isolated by Philipp Assmy), *Fragilariopsis kerguelensis* (R/V *Polarstern* cruise ANT-XXIV/2 in 2008 at 64°S, 0°E, isolated by Philipp Assmy), and the flagellate *Phaeocystis antarctica* (solitary cells isolated by P. Pendoley in March 1992 at 68°39S, 72°21E) were grown at 3°C in semicontinuous dilute cultures in sterile-filtered (0.2 μm) Antarctic seawater (salinity 33.9). The seawater was enriched with trace metals and vitamins according to F/2 medium (Guillard and Ryther 1962). Silicate was added to a concentration of 100 μmol L^{-1}. Nitrate and phosphate were added in concentrations of 100 and 6.25 μmol L^{-1}, reflecting the Redfield N : P ratio of 16 : 1 (Redfield 1958). Experiments were carried out under a light : dark cycle of 16 : 8 h at an incident light intensity of 90 μmol photons m^{-2} s^{-1}. Light intensities were adjusted using a LI-1400 data logger (Li-Cor) with a 4π-sensor (Walz).

Cultures, as well as the respective dilution media, were continuously bubbled through a frit with humidified air of CO_2 partial pressures (P_{CO_2}) of 16.2, 39.5, and 101.3 Pa, resulting in pH values of 8.5, 8.1, and 7.8, respectively (Table 1). CO_2 gas mixtures were generated with gas-mixing pumps (Woesthoff GmbH), using CO_2-free air (Nitrox CO_2 RP280; Domnick Hunter) and pure CO_2 (Air Liquide Germany). Dilutions with the corresponding acclimation media ensured that the pH level remained constant (± 0.03 pH units), cells stayed in the mid-exponential growth phase, and nutrient concentrations were unaffected. Cultures in which the pH shifted significantly (≥ 0.05 units in comparison with cell-free medium at the respective P_{CO_2}) were excluded from further analysis. For the determination of growth rates, cultures were diluted by 1 : 10, followed by daily cell counting until upper cell densities were reached, and then the culture was diluted again. For C_i flux assays, cultures were diluted by 1 : 1 on a daily basis.

Determination of seawater carbonate chemistry—Alkalinity samples were taken from the filtrate (Whatman GFF filter, ~ 0.6 μm), stored in 300 mL borosilicate flasks at 4°C, and measured by potentiometric titration (Brewer et al. 1986). Total alkalinity (TA) was calculated from linear Gran Plots (Gran 1952). pH was measured using a pH meter (Wissenschaftlich-Technische Werkstätten GmbH; model pMX 3000/pH) that was calibrated on a daily basis (2 point calibration) using National Institute of Standards and Technology-certified buffer systems. The carbonate system was calculated from TA, pH, silicate, phosphate, temperature, and salinity using the CO2Sys program (Pierrot et al. 2006). Equilibrium constants of Mehrbach et al. (1973) refitted by Dickson and Millero (1987) were chosen. The parameters of the carbonate system for the respective treatments are given in Table 1.

Growth—Cells were acclimated to culture conditions for ≥ 2 weeks prior to sampling. All cell-count samples were taken at the same time of the day. While cell numbers for

P. antarctica were determined immediately after sampling using a Coulter Multisizer III (Beckmann–Coulter), diatom cell count samples were fixed with 10% acid lugol's solution and stored at 3°C in the dark until counting. Diatom's cell numbers were estimated using a Sedgewick–Rafter Cell S50 (PYSER-SGI) on an inverted microscope (Zeiss Axiovert 200). For each sample, ≥ 400 cells were counted. Cell-specific growth rate (μ) was calculated as

$$\mu = (\ln N_{\text{fin}} - \ln N_0)/\Delta t \quad (1)$$

where N_0 and N_{fin} denote the cell concentrations at the beginning and the end of the experiments, respectively, and Δt is the corresponding duration of incubation in days. As cell-count samples of *F. kerguelensis* were lost, growth rates could not be determined for this species.

Sampling—Cells for bioassays (acclimated to low and high P_{CO_2}) were harvested by gentle filtration over a 3 μm or, in the case of *P. antarctica,* a 1 μm membrane filter (Isopore, Millipore) 4–8 h after the beginning of the photoperiod to allow photosynthesis and CCM activity to be fully induced. Subsequently, the concentrated cells were washed with medium buffered with 50 mmol L^{-1} 2-[4-(2-Hydroxyethyl)-1-piperazinyl]ethanesulfonic acid (HEPES). The samples were then used for measuring C_i fluxes and CA activities with the MIMS. Samples for determination of chlorophyll *a* (Chl *a*) concentration were taken after the measurements and stored at −80°C. Chl *a* was subsequently extracted in 10 mL acetone (overnight in darkness, at 4°C) and determined with a Turner Designs Fluorometer (Model 10-000 R).

Determination of CA activity—Activity of extracellular CA was determined by measuring the loss of ^{18}O from doubly labeled $^{13}C^{18}O_2$ to water caused by the interconversion of CO_2 and HCO_3^- (Silverman 1982). The determination of CA activity was performed with a sector-field multicollector mass spectrometer (Isoprime, GV Instruments) via a gas-permeable polytetrafluoroethylene membrane (PTFE, 0.01 mm) inlet system. The reaction sequence of ^{18}O loss from initial $^{13}C^{18}O^{18}O$ (m/z = 49), via the intermediate $^{13}C^{18}O^{16}O$ (m/z = 47) to the final molecule $^{13}C^{16}O^{16}O$ (m/z = 45) was recorded continuously. The ^{18}O enrichment was calculated as

$$^{18}\text{O log(enrichment)} = \log\frac{(^{13}C^{18}O_2)\times 100}{^{13}CO_2} = \log\frac{(\text{m/z } 49)\times 100}{\text{m/z } 45 + \text{m/z } 47 + \text{m/z } 49} \quad (2)$$

CA measurements were performed in 8 mL of F/2 medium buffered with 50 mmol L^{-1} HEPES (pH 8.0) at 3°C. Chl *a* concentrations in CA assays ranged from 0.03 μg mL^{-1} to 0.60 μg mL^{-1}. To avoid interference with light-dependent C_i uptake by the cells, all measurements were carried out in the dark (Palmqvist et al. 1994). After adding $NaH^{13}C^{18}O_3$ to a final concentration of 1 mmol L^{-1} and chemical equilibration, the uncatalyzed ^{18}O loss was monitored for ~ 20 min prior to the addition of cells. Extracellular CA activity (eCA) was calculated from the increasing rate of ^{18}O depletion after addition of the cells (slope S_2) in comparison with the uncatalysed reaction (slope S_1) and normalized on a Chl *a* basis (Badger and Price 1989):

$$U = \frac{(S_2 - S_1)\times 100}{S_1 \times \mu\text{g Chl } a} \quad (3)$$

Determination of photosynthesis, CO_2, and HCO_3^- uptake—The C_i fluxes were determined during steady-state photosynthesis with the same MIMS as for the CA measurements. The method established by Badger et al. (1994) uses the chemical disequilibrium during light-dependent C_i uptake to differentiate between CO_2 and HCO_3^- fluxes across the plasmalemma. C_i flux estimates are based on simultaneous measurements of O_2 and CO_2 over consecutive light and dark intervals. During dark intervals, known amounts of C_i are added to measure rates as a function of CO_2 and HCO_3^- concentrations. Rates of O_2 consumption in the dark and O_2 evolution in the light provide an estimate of respiration and net C_i fixation, respectively. Net CO_2 uptake is calculated from the steady-state rate of CO_2 depletion at the end of the light period, corrected for the $CO_2 : HCO_3^-$ interconversion in the medium. The HCO_3^- uptake is derived by a mass balance equation (i.e., the difference between net C_i fixation and net CO_2 uptake). Gross CO_2 uptake was calculated from the steady-state rate of CO_2 depletion at the end of the light period and the initial rate of CO_2 generation immediately after the light was turned off. This calculation is based on the assumption that the rate of diffusive CO_2 efflux from a cell in the light represents the rate of CO_2 efflux during the first seconds of the dark phase. All measurements were performed in initially CO_2-free F/2 medium buffered with 50 mmol L^{-1} HEPES (pH 7.8 or 8.1, depending on the treatment) at 3°C. The presence of dextran-bound sulfonamide (150 μmol L^{-1}) ensured the complete inhibition of any eCA activity in all tested species (data not shown). Light and dark intervals during the assay lasted between 10 min and 15 min, depending on equilibration time of the respective C_i addition. The incident photon flux density was 90 μmol photons m^{-2} s^{-1}. Chl *a* concentrations in the assay ranged from 0.11 μg mL^{-1} to 0.93 μg mL^{-1}. Further details on the method and calculations are given in Badger et al. (1994).

Species competition experiments—The role of species competition in structuring phytoplankton communities was tested by growing *C. debilis* (300 ± 58 μm^3) and *P. subcurvata* (163 ± 33 μm^3) in competition at three different P_{CO_2} levels (16.2, 39.5, and 101.3 Pa) without affecting nutrient availability. To mimic different starting conditions for a bloom, where varying cell numbers of species concurrently occur, three different scenarios were chosen with either equal starting abundances for both species (50% : 50%) or a four times higher starting cell number for one or the other species (80% : 20% and vice versa). Initial cell abundance of a species was 1000 : 1000 cells mL^{-1} (50% : 50%), 4000 : 1000 cells mL^{-1} (80% : 20%) or vice versa. At cell densities of ≤ 60.000 cells mL^{-1}, the mixed

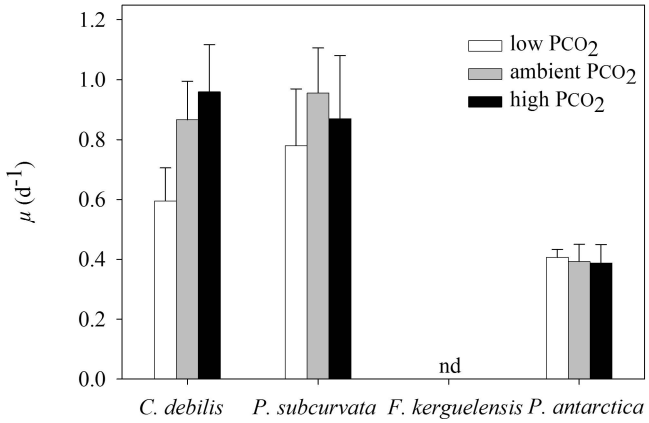

Fig. 1. Growth rates of the tested species acclimated to low, ambient, and high P_{CO_2}. For *Fragilariopsis kerguelensis,* growth rates could not be determined (nd). Values are given in d^{-1} and represent the means of at least triplicate incubations (± SD).

cultures were diluted 1 : 10 with the corresponding acclimation media to avoid shifts in carbonate chemistry and to ensure sufficient supply of nutrients. In any bloom scenario, dilutions were performed twice. Please note that the number of dilutions as well as the dilution rate can influence the final ratio of the two species. Cell numbers were determined using Utermöhl chambers on an inverted microscope (Zeiss Axiovert 200). Each sample was examined until ≥ 400 cells of each species had been counted. Light microscope photographs were taken from the end of experiments showing the final species composition after two dilutions. Theoretical and counted ratios of *C. debilis* : *P. subcurvata* cells were compared at the end of the competition experiments. Theoretical values were based on growth rates obtained in monospecific incubations of the respective P_{CO_2} level.

Results

Growth rates—While growth rates of *C. debilis* significantly increased by 63% from low to high P_{CO_2} (Fig. 1; ANOVA, *F*-test: $p < 0.0001$), values for *P. subcurvata* and *P. antarctica* remained constant independent of the P_{CO_2} (ANOVA, *F*-test: $p > 0.05$). *C. debilis* showed significantly lower growth rates than *P. subcurvata* under low P_{CO_2} (~ 0.6 vs. ~ 0.8 d^{-1}, ANOVA, Bonferroni's multiple-comparison test: $p < 0.01$), but reached similar high values under ambient and high P_{CO_2} (~ 0.9–1.0 d^{-1}, ANOVA, Bonferroni's multiple-comparison test: $p > 0.05$). Among the investigated species, *P. antarctica* displayed the lowest growth rates with ~ 0.4 d^{-1}.

Photosynthesis and C_i fluxes—Rates of photosynthetic O_2 evolution (CO_2 as well as HCO_3^- uptake), being measured as a function of C_i availability, differed substantially depending on species as well as acclimation P_{CO_2} (Table 2). The half-saturation concentration ($K_{1/2}$) of CO_2 for photosynthesis was generally very low, being < 2 μmol CO_2 L^{-1} for all species. The V_{max} for photosynthesis remained constant in *C. debilis* (*t*-test, $t = 2.235$, df = 4, $p = 0.0891$) and *P. antarctica* (*t*-test, $t = 0.2877$, df = 4, $p = 0.7879$), while the V_{max} changed in response to P_{CO_2} in *P. subcurvata* (*t*-test, $t = 6.824$, df = 4, $p = 0.0024$) and *F. kerguelensis* (*t*-test, $t = 6.235$, df = 4, $p = 0.0034$). While for *P. subcurvata,* V_{max} of photosynthesis decreased with increasing P_{CO_2}, the opposite trend was observed for *F. kerguelensis.*

The $K_{1/2}$ values for gross CO_2 uptake remained unaltered in response to P_{CO_2} except for *P. antarctica,* for which the $K_{1/2}$ values significantly decreased with increasing P_{CO_2} (Table 2; *t*-test, $t = 3.098$, df = 4, $p = 0.0363$). The V_{max} values were enhanced under elevated P_{CO_2} in *F. kerguelensis* (*t*-test, $t = 7.235$, df = 4, $p = 0.0019$), while in

Table 2. $K_{1/2}$ and V_{max} values for photosynthesis and gross and net CO_2 uptake, as well as HCO_3^- uptake, were determined for *Chaetoceros debilis, Pseudo-nitzschia subcurvata, Fragilariopsis kerguelensis,* and *Phaeocystis antarctica* acclimated to low and high P_{CO_2}. Kinetic parameters were calculated from a Michaelis–Menten fit to the combined data of at least three independent measurements. Values for $K_{1/2}$ and V_{max} are given in μmol L^{-1} and μmol (mg Chl *a*)$^{-1}$ h^{-1}, respectively. A dash indicates that values could not be determined.

	Photosynthesis		Gross CO_2 uptake		Net CO_2 uptake		HCO_3^- uptake	
P_{CO_2}	$K_{1/2}$	V_{max}	$K_{1/2}$	V_{max}	$K_{1/2}$	V_{max}	$K_{1/2}$	V_{max}
C. debilis								
Low	1.43±0.1	258±15	1.8±1.1	119±27	0.7±0.5	106±16	77±29	152±12
High	1.56±0.2	234±11	2.7±0.7	164±16	2.0±1.1	91±24	216±35	143±8
P. subcurvata								
Low	1.76±0.2	231±7	3.2±0.4	158±7	3.2±1.1	88±9	172±20	146±7
High	1.19±0.2	192±7	2.6±0.6	135±8	0.8±1.4	111±8	200±85	88±11
F. kerguelensis								
Low	1.83±0.2	169±9	4.2±1.4	42±6	—	—	42±55	173±11
High	1.88±0.4	223±12	3.8±1.5	87±9	—	—	53±24	244±15
P. antarctica								
Low	0.74±0.1	219±8	1.0±0.1	167±8	0.9±0.1	153±5	226±16	65±4
High	0.01±0.3	217±9	0.6±0.1	143±5	—	145±10	—	74±10

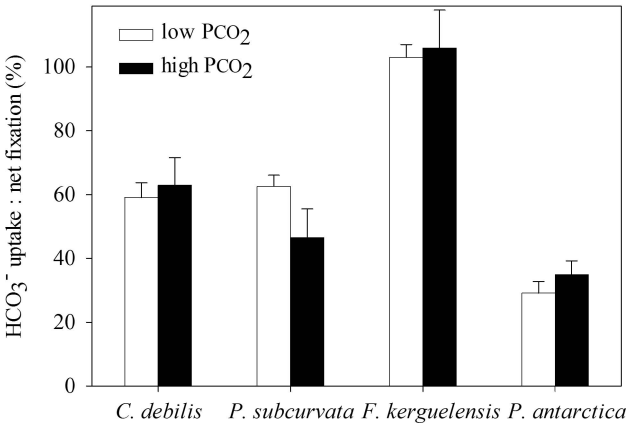

Fig. 2. Ratios of HCO_3^- uptake: net fixation of the tested species acclimated to low and high P_{CO_2}. Ratios from membrane inlet mass spectrometry (MIMS) measurements were based on the rates obtained at C_i concentrations of about 2 mmol L^{-1}. Values represent the means of triplicate incubations (± SD).

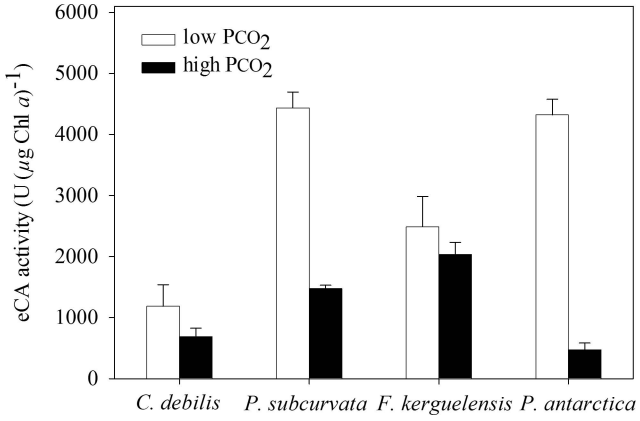

Fig. 3. Chl *a*-specific activities of eCA from the tested species acclimated to low and high P_{CO_2}. Values represent the means of triplicate incubations (± SD).

P. subcurvata (*t*-test, $t = 3.907$, df = 4, $p = 0.0174$) and *P. antarctica* (*t*-test, $t = 4.407$, df = 4, $p = 0.0116$) they were reduced under these conditions (Table 2). Only in *C. debilis,* the V_{max} values remained unaltered by P_{CO_2} (*t*-test, $t = 2.531$, df = 4, $p = 0.0646$).

For net CO_2 uptake, $K_{1/2}$ and V_{max} values did not change in response to P_{CO_2} in the tested species (Table 2) except for *P. subcurvata,* in which the V_{max} values significantly increased under elevated P_{CO_2} (*t*-test, $t = 3.308$, df = 4, $p = 0.0297$). In *F. kerguelensis,* net CO_2 uptake rates were very low and hence no $K_{1/2}$ and V_{max} values could be estimated. Among the investigated species, *P. antarctica* obtained highest V_{max} values for net CO_2 uptake. Regarding $K_{1/2}$ determinations, they could only be derived for low P_{CO_2} acclimated cells.

In terms of HCO_3^- uptake, $K_{1/2}$ values remained constant in *P. subcurvata* and *F. kerguelensis* (Table 2), whereas values increased with increasing P_{CO_2} in *C. debilis* (*t*-test, $t = 5.297$, df = 4, $p = 0.0061$). In *P. antarctica,* $K_{1/2}$ could not be determined for high P_{CO_2}. Except for *C. debilis* and *P. antarctica,* V_{max} for HCO_3^- uptake changed significantly in response to P_{CO_2}. While V_{max} of *F. kerguelensis* significantly increased by 41% from low to high P_{CO_2} (*t*-test, $t = 6.611$, df = 4, $p = 0.0027$), V_{max} of *P. subcurvata* was reduced by 40% under the same conditions (*t*-test, $t = 7.705$, df = 4, $p = 0.0015$). In comparison with the other species, *P. antarctica* displayed lowest V_{max} values at the tested P_{CO_2} levels.

The contribution of HCO_3^- uptake relative to net fixation was not affected by the different P_{CO_2} acclimations, even though species differed strongly in their preferred carbon source (Fig. 2). With values of ~ 100%, the preference for HCO_3^- in *F. kerguelensis* was highest, whereas in *P. antarctica* values of ~ 30% reflected a strong preference for CO_2. For *C. debilis* and *P. subcurvata,* both carbon sources contributed equally to net fixation, values ranged between 59% and 63% in *C. debilis* and between 63% and 47% in *P. subcurvata* at low and high P_{CO_2}, respectively (Fig. 2).

Extracellular CA activity—Activities of eCA were exceptionally high in all tested species and conditions (Fig. 3). eCA activities ranged between 1189 ± 349 and 4433 ± 264 U (µg Chl *a*)$^{-1}$ under low P_{CO_2} and 478 ± 108 and 2034 ± 195 U (µg Chl *a*)$^{-1}$ under high P_{CO_2}. In *C. debilis* and *F. kerguelensis,* eCA activities remained unaffected by P_{CO_2}, while they were strongly down-regulated in *P. subcurvata* (*t*-test, $t = 24.52$, df = 8, $p < 0.0001$) and *P. antarctica* (*t*-test, $t = 23.58$, df = 4, $p < 0.0001$) with increasing P_{CO_2}.

Species competition experiments—For all starting scenarios, the abundance of *C. debilis* relative to *P. subcurvata* increased with increasing P_{CO_2} (Figs. 4, 5; ANOVA, *F*-test: $p < 0.05$). In the 50% : 50% and 80% : 20% treatments, the counted final cell numbers of *C. debilis* relative to *P. subcurvata* generally did not differ significantly from the theoretical values (Fig. 5). The only exception was observed under ambient P_{CO_2} of the 80% : 20% treatment because the counted ratio was significantly lower than the theoretical value (*t*-test, $t = 8.962$, df = 8, $p = 0.0009$). In case *P. subcurvata* had a higher starting number (20% : 80%), the relative contribution of *C. debilis* to *P. subcurvata* was significantly reduced compared with theoretical values at all tested P_{CO_2} levels (low P_{CO_2}: *t*-test, $t = 3.674$, df = 4, $p = 0.0213$; ambient P_{CO_2}: *t*-test, $t = 8.649$, df = 4, $p = 0.0010$; high P_{CO_2}: *t*-test, $t = 5.095$, df = 4, $p = 0.0070$).

Except for the 80% : 20% treatment grown under ambient P_{CO_2} (*t*-test, $t = 4.181$, df = 4, $p = 0.0139$), growth rates of *C. debilis* in mixed cultures remained unaltered before and after the first dilution in the 50% : 50% and 80% : 20% treatments (Fig. 6). When *P. subcurvata* had a higher starting number (20% : 80%), growth rates of *C. debilis* were strongly reduced after dilution compared with values estimated before dilution (low p_{CO_2}: *t*-test, $t = 3.222$, df = 4, $p = 0.0322$; ambient p_{CO_2}: *t*-test, $t = 3.569$, df = 4, $p = 0.0234$; high p_{CO_2}: *t*-test, $t = 3.122$, df = 4, $p = 0.0354$).

Discussion

The present study investigates four Antarctic phytoplankton key species in terms of their CO_2 sensitivity in

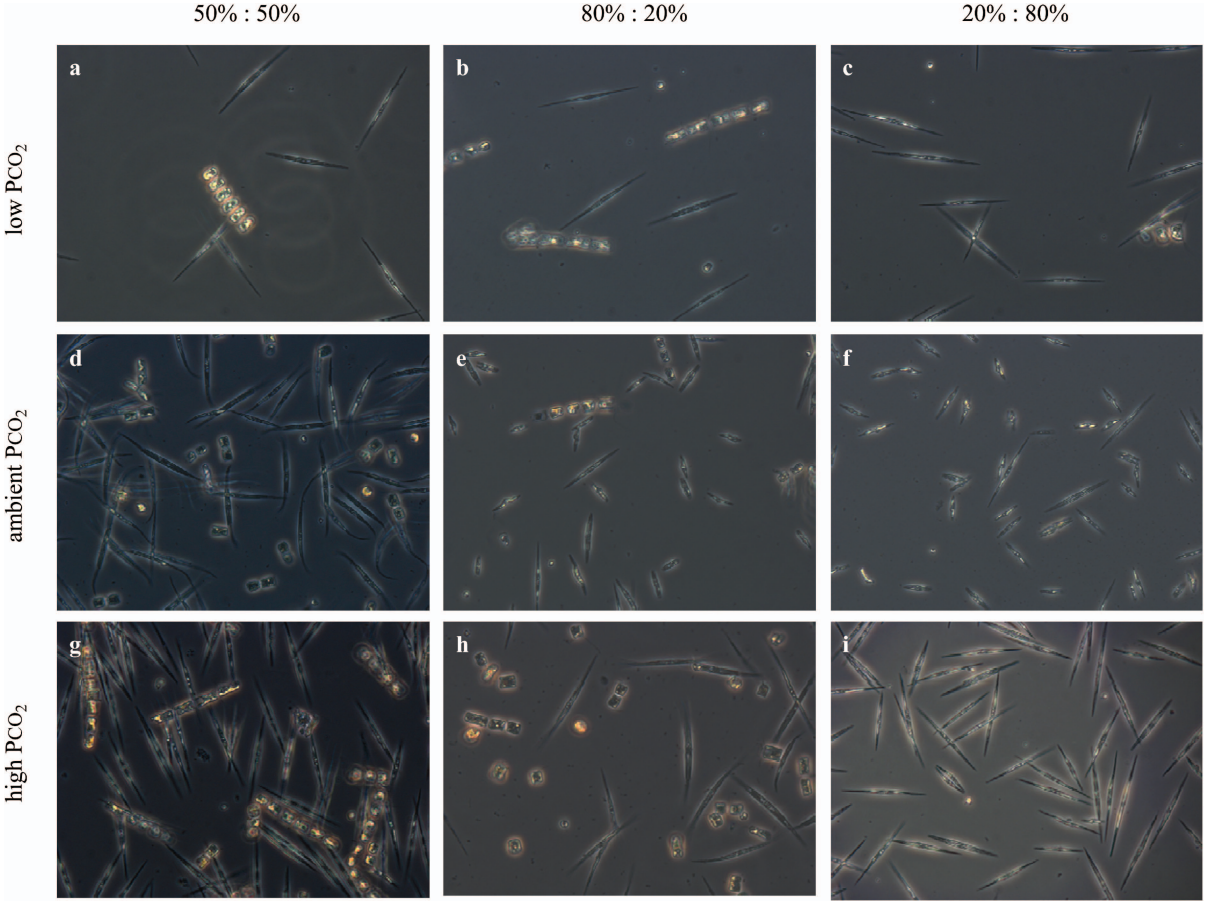

Fig. 4. Light microscope photographs from species competition experiments, in which *Chaetoceros debilis* and *Pseudo-nitzschia subcurvata* were grown in competition at (a, b, c) low, (d, e, f) ambient, and (g, h, i), high P_{CO_2}. To simulate different bloom conditions, initial ratios of cell abundances were (a, d, g) 50% *C. debilis* : 50% *P. subcurvata* (50 : 50%), (b, e, h) 80% *C. debilis* : 20% *P. subcurvata* (80 : 20%), or (c, f, i) 20% *C. debilis* : 80% *P. subcurvata* (20 : 80%). Photographs were taken at the end of experiments, showing the final species composition after two dilutions.

growth and inorganic carbon acquisition. Our study indicates that only the growth of *C. debilis* was sensitive to the applied P_{CO_2} levels. In all tested species, very efficient CCMs were observed, but the degree in CO_2-dependent regulation of the preferred C_i source and their uptake kinetics, as well as extracellular CA activities, varied. Species competition experiments with *C. debilis* and *P. subcurvata* confirmed the CO_2-stimulated growth of *C. debilis* in presence of *P. subcurvata*.

Growth—Cell division rates in our study are similar to values determined in previous studies on the growth of Antarctic phytoplankton under present-day CO_2 concentrations. Fiala and Oriol (1990) estimated values of $\sim$ 0.6 d^{-1} for the polar *Chaetoceros deflandrei*. Similar rates were determined for *Chaetoceros* cf. *neogracile* (Gleitz et al. 1996). For *Pseudo-nitzschia* sp. growth rates were $\sim$ 0.5 d^{-1} (McMinn et al. 2005), while for *P. antarctica* growth varied between 0.1 d^{-1} and 0.3 d^{-1}, depending on the strain tested (Moisan and Mitchell 1999; Kropuenske et al. 2010).

In response to increasing P_{CO_2}, growth rates of *C. debilis* were stimulated by 63%, whereas growth of *P. subcurvata* and *P. antarctica* did not change significantly (Fig. 1). In a study on temperate diatom species, Burkhardt et al. (1999) reported CO_2-sensitive growth only for some species at very low CO_2 concentrations, ranging from $\sim$ 2 μmol kg^{-1} to 6 μmol kg^{-1} CO_2. In a similar CO_2 range, the polar diatom *Rhizosolenia* cf. *alata* also was found to have enhanced growth rates with increasing CO_2 (Riebesell et al. 1993). In contrast, Ihnken et al. (2011) showed that growth rates of the temperate diatom *Chaetoceros muelleri* decreased when cells were exposed to increasing CO_2 concentrations, ranging between 11 μmol L^{-1} and 75 μmol L^{-1} CO_2. This CO_2 effect was only observed under low light ($\leq$ 50 μmol photons m^{-2} s^{-1}), and not under high light ($\geq$ 100 μmol photons m^{-2} s^{-1}) conditions. Experiments with the polar diatom *Chaetoceros brevis* (Boelen et al. 2011) and *Proboscia alata* (Hoogstraten et al. 2012) indicated no change in growth in response to P_{CO_2}, ranging between 13 Pa and 76 Pa. Ship-board incubation experiments with natural phytoplankton communities showed CO_2-dependent shifts within diatoms from pennate diatoms such as *Cylindrotheca* or *Pseudo-nitzschia*, which dominated under low and ambient P_{CO_2}, toward the centric diatom *Chaetoceros* under high P_{CO_2} (Tortell et al. 2008*b;* Feng et al. 2010). Our results are in line with these studies.

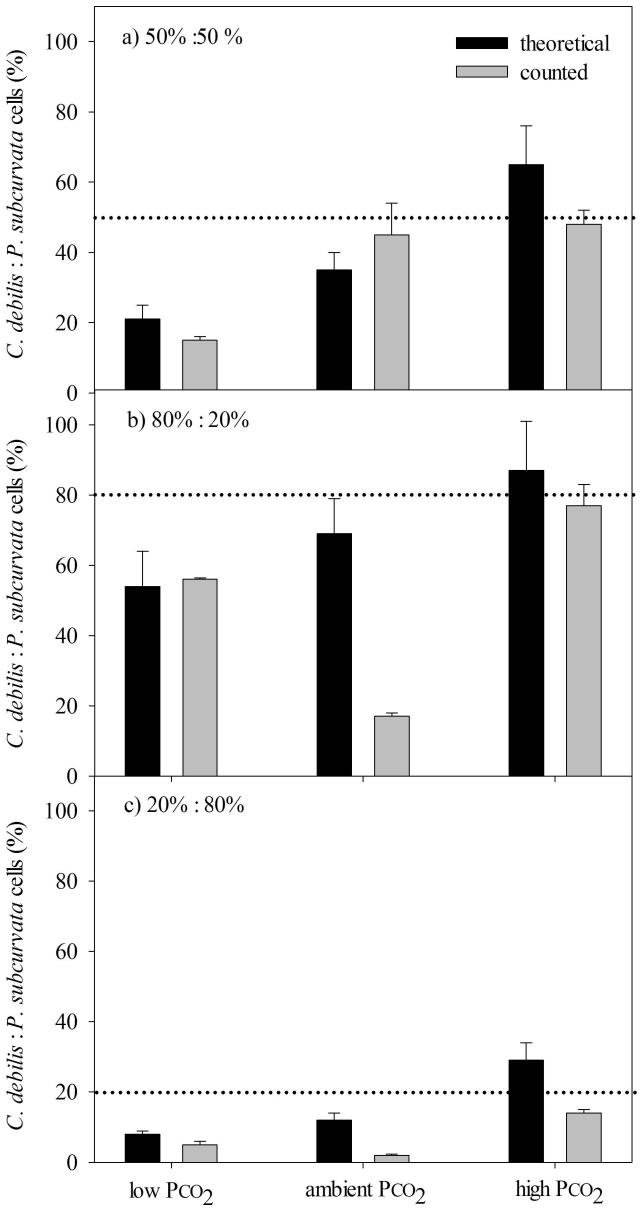

Fig. 5. Theoretical and counted ratios of *C. debilis* : *P. subcurvata* cells at the end of the competition experiments of the respective P_{CO_2} level. Theoretical values were based on growth rates obtained in monospecific incubations. Final values represent the means of triplicate incubations (± SD). The dotted lines indicate the proportion of *C. debilis* relative to *P. subcurvata* cells at the start of the experiments.

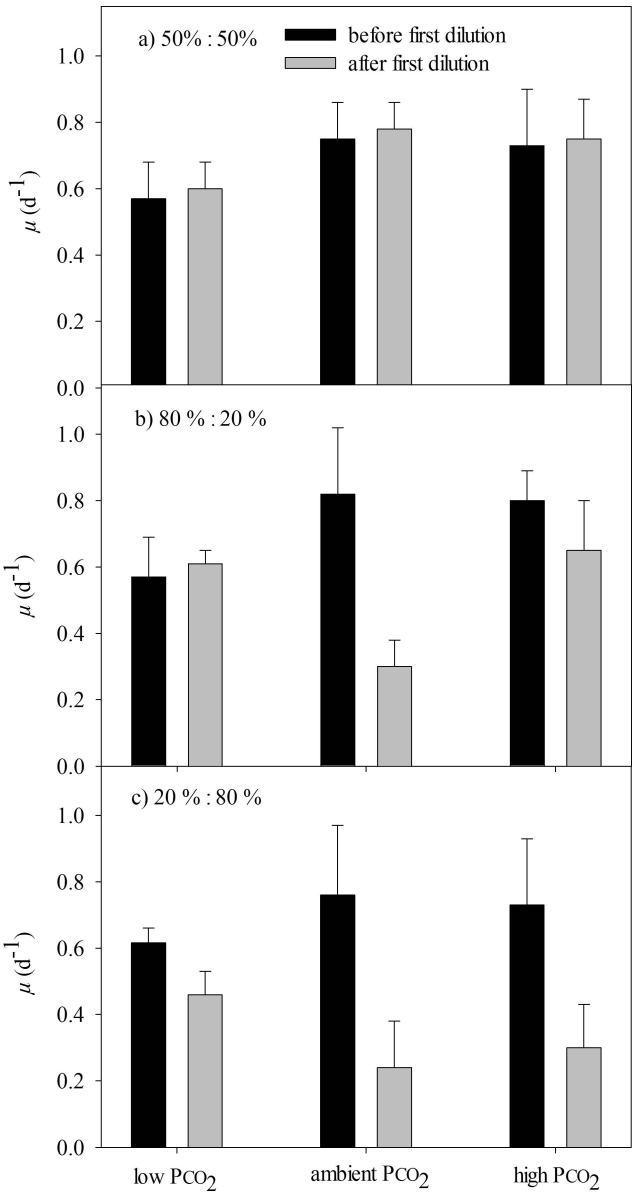

Fig. 6. Growth rates of *C. debilis* determined before and after the first dilution of the species competition experiments of the respective P_{CO_2} level. Values are given in d^{-1} and represent the means of triplicate incubations (± SD).

Overall, we conclude that *P. subcurvata* is able to maintain high growth rates over the tested P_{CO_2} levels, while high P_{CO_2} promotes the growth of *C. debilis*. These findings indicate that some *Chaetoceros* species may benefit from ongoing ocean acidification.

CO_2 sensitivity of CCM components—The mode of carbon acquisition determines, to a large extent, how sensitive phytoplankton respond to changes in P_{CO_2}. The CO_2 sensitivity in photosynthesis is mainly the result of both the slow maximum turnover rate and the poor affinity of RubisCO for its substrate (K_M of ~ 20–70 μmol L^{-1} for marine phytoplankton and ~ 30–40 μmol L^{-1} for diatoms). In our experiments, $K_{1/2}$ (CO_2) values for photosynthesis were < 2 μmol CO_2 L^{-1} in all tested species (Table 2), indicating the operation of very efficient CCMs. These $K_{1/2}$ (CO_2) values are comparable to those reported for various temperate phytoplankton species (Colman and Rotatore 1995; Burkhardt et al. 2001). Mitchell and Beardall (1996) obtained a $K_{1/2}$ (CO_2) value of ~ 1 μmol L^{-1} at pH 7.5 in the sea-ice diatom *Nitzschia frigida*. In all species, $K_{1/2}$ (CO_2) values for photosynthesis remained unaltered by P_{CO_2} (Table 2). While most studies showed an up-regulation in $K_{1/2}$ values for photosynthesis with increasing P_{CO_2}, it was also observed that some

species, such as the temperate diatom *Eucampia zodiacus* or the flagellate *Phaeocystis globosa,* did not change their affinities under these conditions (Rost et al. 2003; Trimborn et al. 2008, 2009). Our results demonstrate that all tested Antarctic species operate very efficient and yet constitutively expressed CCMs. The efficiency of a CCM results from the interplay of various components of the CCM, such as C_i sources and extracellular CA activities, these components will be discussed in the following section.

As in previous studies on SO phytoplankton (Cassar et al. 2004; Tortell et al. 2008*a*; Neven et al. 2011), simultaneous uptake of CO_2 and HCO_3^- was present in all tested species (Fig. 2; Table 2). However, there were large species-specific differences in the preferred C_i source. Irrespective of the P_{CO_2} during acclimation, *F. kerguelensis* predominantly took up HCO_3^-, while *P. antarctica* was characterized by a strong preference for CO_2. In response to increasing P_{CO_2}, *C. debilis* and *P. subcurvata* used CO_2 and HCO_3^- in equal quantities. In agreement with Cassar et al. (2004) and Neven et al. (2011), our results confirm a high variability in terms of the preferred C_i source among Antarctic phytoplankton (Fig. 2), while Tortell et al. (2008*a*, 2010) determined HCO_3^- as the main C_i source in most phytoplankton assemblages from the Ross Sea. Even though the preferred C_i source seems to differ among Antarctic phytoplankton, a clear relationship between the species composition and a preferred C_i source could not yet be established (Tortell et al. 2008*a*, 2010; Neven et al. 2011). Reasons for this might be due to the assay pH, at which the C_i source is determined. For instance, the ^{14}C disequilibrium technique is often applied in field studies using an assay pH of 8.5, which in most cases differs from the in situ pH values (Tortell et al. 2010; Neven et al. 2011). One may hypothesize that the C_i uptake behavior strongly depends on the assay pH. To potentially circumvent this pH effect, our MIMS measurements on C_i sources were conducted either with an assay pH of 7.8 or 8.1, depending on the respective P_{CO_2} treatment. Even though we cannot exclude biases imposed by the pH during our measurements (pH values do not fully correspond to the acclimation pH), our results clearly point toward species-specific differences in CO_2 and HCO_3^- use in Antarctic phytoplankton.

The enzyme eCA represents an important component of the CCM as it catalyzes the equilibration between HCO_3^- and CO_2. For the tested Antarctic phytoplankton species, eCA activities were extremely high, ranging from ~ 1200 U to ~ 4500 U per μg Chl *a* under low P_{CO_2} and from ~ 500 U to ~ 2000 U per μg Chl *a* under high P_{CO_2} (Fig. 3). The magnitude of our eCA estimates is similar to or higher than values determined in Antarctic natural phytoplankton communities, ranging between ~ 100 U and ~ 1000 U per μg Chl *a* at P_{CO_2} levels from ~ 10 Pa to ~ 40 Pa (Tortell et al. 2008*a*, 2010). In particular under elevated P_{CO_2}, our measured eCA activities are remarkably high in comparison with eCA activities observed in temperate diatoms (~ 50–150 U per μg Chl *a*; Burkhardt et al. 2001; Rost et al. 2003; Trimborn et al. 2009). We suggest that polar species require high eCA activities also at elevated P_{CO_2} to compensate for the very slow CO_2 diffusion and interconversion between HCO_3^- and CO_2 prevailing under low temperatures.

In our study, a strong down-regulation of eCA activities was found under elevated P_{CO_2} in *P. subcurvata* and *P. antarctica,* while eCA activities of *C. debilis* and *F. kerguelensis* were constitutively expressed (Fig. 3). In response to increasing P_{CO_2}, eCA activities of *Phaeocystis globosa* remained unaffected, whereas those of temperate diatoms were usually strongly down-regulated (Burkhardt et al. 2001; Rost et al. 2003; Trimborn et al. 2009). In natural phytoplankton assemblages, only few studies reported a down-regulation of eCA activities with increasing P_{CO_2} (Berman-Frank et al. 1994; Tortell et al. 2006), while in Antarctic phytoplankton eCA activities appear to be constitutively expressed (Tortell et al. 2008*a*, 2010; Neven et al. 2011).

The reason that eCA activities are up-regulated with decreasing P_{CO_2} is still controversially debated. One common notion is that eCA supplies CO_2 from the large HCO_3^- pool to the CO_2 uptake systems (Badger and Price 1994). Such a function of eCA could apply especially for large phytoplankton cells because they are more prone to CO_2 shortage in their diffusive boundary layer (Wolf-Gladrow and Riebesell 1997). Previous studies also reported, in particular for diatoms, a strong correlation between predominant HCO_3^- uptake and higher eCA activities, while diatoms lacking eCA activity typically prefer CO_2 (Martin and Tortell 2008; Trimborn et al. 2008). Based on these observations, Trimborn et al. (2008) proposed that eCA serves to recycle CO_2 by converting the CO_2 leaking out of the cell to HCO_3^- that is subsequently taken up by HCO_3^- transporters. It was also suggested that eCA is linked with the HCO_3^- transporter.

The results for *P. subcurvata* are in line with this hypothesis because eCA activities correlated positively with the preference for HCO_3^- uptake in response to decreasing P_{CO_2} (Figs. 2, 3). This hypothesis holds true also for *C. debilis* and *F. kerguelensis* because, independent of the P_{CO_2}, constant and high eCA activities correlated with constant and predominant HCO_3^- uptake. This hypothesis is not supported, however, by the data of *P. antarctica* because predominant CO_2 uptake did not correlate with low and constant eCA activities (Figs. 2, 3). It appears that the proposed C_i recycling mechanism by Trimborn et al. (2008) mainly applies for diatoms. To sum up the present findings, very high eCA activities were found in the tested Antarctic species, but strong species-specific differences in its regulation existed. Due to the cold temperatures in polar regions, and therefore a low CO_2 diffusion and interconversion between HCO_3^- and CO_2, we conclude that high eCA activities are of particular importance for polar species.

Role of species competition in structuring phytoplankton communities—To test species interactions, we grew *C. debilis* and *P. subcurvata* in mixed cultures at different P_{CO_2} levels. These species were found to have successful strategies to form prominent blooms (Arrigo et al. 1999; Assmy and Smetacek 2009). Different from a bloom situation in nature, in which multiple parameters change

over the course of the bloom (P_{CO_2}, nutrients, light), we followed a semicontinuous dilute culturing approach to ensure constant seawater carbonate chemistry without affecting nutrient availability, in order to study solely the effect of P_{CO_2}. In accordance with our results on the CO_2-dependent stimulation in growth of *C. debilis* in monocultures (Fig. 1), the contribution of *C. debilis* relative to *P. subcurvata* cells increased with increasing P_{CO_2} also in mixed cultures (Fig. 4). Under low P_{CO_2}, however, *P. subcurvata* dominates all bloom scenarios, except for the 80% *C. debilis* : 20% *P. subcurvata* treatment (Fig. 4). This is in agreement with its growth rates obtained in monoculture experiments at low P_{CO_2} (Fig. 1), suggesting that this species copes better than *C. debilis* under these conditions.

Except for the 50% *C. debilis* : 50% *P. subcurvata* treatment at ambient P_{CO_2}, final cell numbers of *C. debilis* relative to *P. subcurvata* were either similar or reduced compared with theoretical values, which were calculated using the growth rates obtained in monocultures (Fig. 5). The strongest reduction of *C. debilis* relative to *P. subcurvata* cells was observed in all 20% *C. debilis* : 80% *P. subcurvata* treatments. Please note that in this bloom scenario, growth rates for *C. debilis* determined before the first dilution (Fig. 6c) were similar to growth rates obtained in monoculture experiments (Fig. 1). After dilution, however, growth rates of *C. debilis* in mixed cultures were strongly reduced (Fig. 6c). Considering further that in all 50% *C. debilis* : 50% *P. subcurvata* treatments, growth rates of *C. debilis* remained unaltered before and after dilution (Fig. 6a), indicating that the dilution itself did not affect growth rates in *C. debilis*. Because of this, we argue that the reduced growth rates of *C. debilis* observed in all 20% *C. debilis* : 80% *P. subcurvata* treatments were related to some other effect. One explanation could be the production of allelochemicals by *P. subcurvata* induced by the presence of *C. debilis*. Such an effect presumably depends upon the cell density of *P. subcurvata* and would explain why it is only observed in the 20% *C. debilis* : 80% *P. subcurvata* treatment.

Evidence for the presence of allelopathic interactions among the group of diatoms exists for the temperate diatom *Skeletonema costatum* (Yamasaki et al. 2010). Even though still speculative and not conclusively answered here, we suggest that *P. subcurvata* may be a candidate that excretes allelochemicals, providing competitive advantage over *C. debilis* and potentially other diatom species. Future experiments are needed to evaluate further the potential role of allelochemicals in *P. subcurvata* and its effect on other phytoplankton species. Taking into account that our species competition experiments were conducted under nutrient-replete conditions, which are not representative for the largely iron-limited SO, future experiments also need to consider nutrient limitation, in particular iron, and how this might influence species interactions and therefore phytoplankton succession.

Ecological implications and conclusions—C. debilis and *P. subcurvata* are so-called boom-and-bust bloomers. They out-compete others due to their high intrinsic growth rates and are able to build up high biomass and thus strongly contribute to carbon export (Smetacek et al. 2004). *C. debilis* blooms are usually observed during spring time while *P. subcurvata* forms blooms in summer (Thomson et al. 2006). During spring P_{CO_2}, macro- and micronutrients are usually high. In agreement, our results demonstrate that *C. debilis* obtained highest growth rates under ambient and high P_{CO_2} levels (Fig. 1). In comparison, *P. subcurvata* thrives much better under low CO_2 conditions (Fig. 1), a finding that correlates with its occurrence in summertime when seawater P_{CO_2} is lowered from previous spring blooms. This characteristic, together with its trait to potentially produce allelochemicals, may allow *P. subcurvata* to cope best under summer conditions.

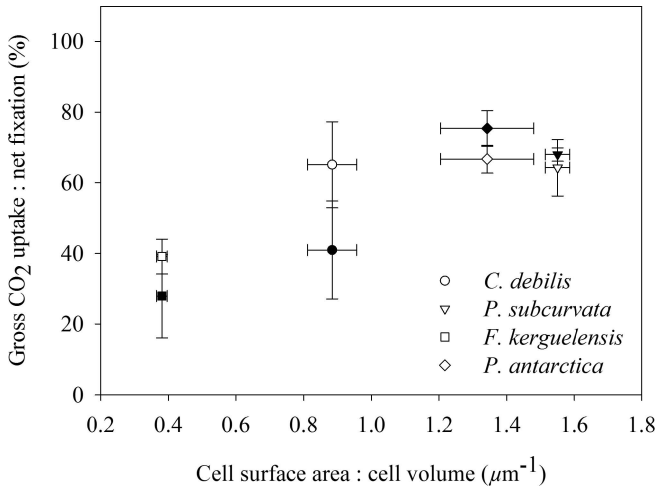

Fig. 7. The contribution of gross CO_2 uptake relative to net fixation (%) plotted against the cell surface (A) area to cell volume (V) ratio of single cells of *C. debilis*, *P. subcurvata*, *F. kerguelensis,* and *P. antarctica*. Closed and open symbols denote the acclimation of the respective species to low P_{CO_2} and high P_{CO_2}, respectively. A : V ratios were calculated of single cells according to Hillebrand et al. (1999).

In view of the ongoing acidification of the oceans, *C. debilis* seems to benefit most from the predicted changes because it was the only species showing stimulation in growth (Fig. 1). Considering that all species displayed very efficient CCMs, the question arises why growth of *C. debilis* is particularly sensitive to P_{CO_2}. For instance, *C. debilis* may benefit from increased diffusive CO_2 uptake and/or reduced energetic costs of the CCM under elevated P_{CO_2}. The latter could be the result of reduced leakage due to a smaller outward CO_2 gradient under elevated P_{CO_2} (e.g., Raven and Lucas 1985; Trimborn et al. 2008). According to our results, however, the loss of CO_2 through leakage determined during C_i flux measurements via MIMS was similarly high for all species (data not shown) and therefore can be excluded as an explanation. A higher diffusive CO_2 uptake, on the other hand, should be reflected in higher gross CO_2 uptake rates and potentially correlate with the cell surface (A) area to volume (V) ratio. The contribution of gross CO_2 uptake relative to net fixation of the tested species was found to increase as their A : V ratio increased (Fig. 7). In comparison, *F. kerguelensis* had the lowest A : V

ratio, a finding that correlated with its preference for HCO_3^- (Fig. 2). The other species had generally higher A : V ratios, as well as a higher contribution of gross CO_2 uptake (Fig. 2; Table 2). Nonetheless, *C. debilis* did not show a significant increased contribution of gross CO_2 uptake at elevated P_{CO_2} (Fig. 7) and therefore cannot explain its CO_2 sensitivity.

In conclusion, there might be other CO_2-dependent aspects than C_i acquisition that cause the increase in growth in this species, which should be included in future studies on ocean acidification responses. As shown in the species competition experiments, future studies should also encompass species interaction because they can counteract species-specific physiological responses through allelopathic interactions.

Acknowledgments

We thank two anonymous reviewers who helped to improve the quality of the manuscript.

This work was funded by the German Science Foundation (DFG) project TR 899, and by the European Research Council (ERC) under the European Community's Seventh Framework Programme (FP7 / 2007–2013), ERC grant agreement 205150.

References

Arrigo, K. R., D. H. Robinson, D. L. Worthen, R. B. Dunbar, G. R. DiTullio, M. van Woert, and M. P. Lizotte. 1999. Phytoplankton community structure and the drawdown of nutrients and CO_2 in the Southern Ocean. Science **283:** 365–367, doi:10.1126/science.283.5400.365

Assmy, P., and V. Smetacek. 2009. Algal blooms, p. 27–41. *In* M. Schaechter [ed.], Encyclopedia of microbiology. Elsevier.

Badger, M. R., K. Palmqvist, and J.-W. Yu. 1994. Measurement of CO_2 and HCO_3^- fluxes in cyanobacteria and microalgae during steady-state photosynthesis. Physiol. Plant. **90:** 529–536, doi:10.1111/j.1399-3054.1994.tb08811.x

———, and G. D. Price. 1989. Carbonic anhydrase activity associated with the cyanobacterium *Synechococcus* PCC7942. Plant Physiol. **89:** 51–60, doi:10.1104/pp.89.1.51

———, and ———. 1994. The role of carbonic anhydrase in photosynthesis. Annu. Rev. Plant Physiol. Plant Mol. Biol. **45:** 369–92, doi:10.1146/annurev.pp.45.060194.002101

Berman-Frank, I., T. Zohary, J. Erez, and Z. Dubinsky. 1994. CO_2 availability, carbonic anhydrase and the annual dinoflagellate bloom in Lake Kinneret. Limnol. Oceanogr. **39:** 1822–1834, doi:10.4319/lo.1994.39.8.1822

Boelen, P., W. H. van de Poll, H. J. van der Strate, I. A. Neven, J. Beardall, and A. G. J. Buma. 2011. Neither elevated nor reduced CO_2 affects the photophysiological performance of the marine Antarctic diatom *Chaetoceros brevis*. J. Exp. Mar. Biol. Ecol. **406:** 38–45, doi:10.1016/j.jembe.2011.06.012

Brewer, P. G., A. L. Bradshow, and R. T. Williams. 1986. Measurement of total carbon dioxide and alkalinity in the north Atlantic Ocean in 1981, p. 358–381. *In* J. R. Trabalka and D. E. Reichle [eds.], The changing carbon cycle—a global analysis. Springer.

Burkhardt, S., G. Amoroso, U. Riebesell, and D. Sültemeyer. 2001. CO_2 and HCO_3^- uptake in marine diatoms acclimated to different CO_2 concentrations. Limnol. Oceanogr. **46:** 1378–1391, doi:10.4319/lo.2001.46.6.1378

———, U. Riebesell, and I. Zondervan. 1999. Effects of growth rate, CO_2 concentration, cell size on the stable carbon isotope fractionation in marine phytoplankton. Geochim. Cosmochim. Acta **63:** 3729–3741, doi:10.1016/S0016-7037(99)00217-3

Cassar, N., E. A. Laws, R. R. Bidigare, and B. N. Popp. 2004. Bicarbonate uptake by Southern Ocean phytoplankton. Glob. Biogeochem. Cycles **18:** GB2003, doi:10.1029/2003GB002116

Colman, B., and C. Rotatore. 1995. Photosynthetic inorganic carbon uptake and accumulation in two marine diatoms. Plant. Cell Environ. **18:** 919–924, doi:10.1111/j.1365-3040.1995.tb00601.x

Dickson, A. G., and F. J. Millero. 1987. A comparison of the equilibrium constants for the dissociation of carbonic acid in seawater media. Deep-Sea Res. **34:** 1733–1743, doi:10.1016/0198-0149(87)90021-5

Feng, Y., and others. 2010. Interactive effects of iron, irradiance and CO_2 on Ross Sea phytoplankton. Deep-Sea Res. Part I **57:** 368–383, doi:10.1016/j.dsr.2009.10.013

Fiala, M., and L. Oriol. 1990. Light–temperature interactions on the growth of Antarctic diatoms. Polar Biol. **10:** 629–636, doi:10.1007/BF00239374

Giordano, M., J. Beardall, and J. A. Raven. 2005. CO_2 concentrating mechanisms in algae: Mechanisms, environmental modulation, and evolution. Annu. Rev. Plant Biol. **56:** 99–131, doi:10.1146/annurev.arplant.56.032604.144052

Gleitz, M., H. Kukert, U. Riebesell, and G. S. Dieckmann. 1996. Carbon acquisition and growth of Antarctic sea ice diatoms in closed bottle incubations. Mar. Ecol. Prog. Ser. **135:** 169–177, doi:10.3354/meps135169

Gran, G. 1952. Determinations of the equivalence point in potentiometric titrations of seawater with hydrochloric acid. Oceanol. Acta **5:** 209–218.

Guillard, R. R. L., and J. H. Ryther. 1962. Studies of marine planktonic diatoms. Can. J. Microbiol. **8:** 229–239, doi:10.1139/m62-029

Hansen, P. J. 2002. Effect of high pH on the growth and survival of marine phytoplankton: Implications for species succession. Aquat. Microb. Ecol. **28:** 279–288, doi:10.3354/ame028279

Hillebrand, H., C.-D. Dürselen, D. Kirschtel, U. Pollingher, and T. Zohary. 1999. Biovolume calculation for pelagic and benthic microalgae. J. Phycol. **35:** 403–424, doi:10.1046/j.1529-8817.1999.3520403.x

Hoogstraten, A., K. R. Timmermans, and H. J. W. de Baar. 2012. Morphological and physiological effects in *Proboscia alata* (Bacillariophyceae) grown under different light and CO_2 conditions of the modern Southern Ocean. J. Phycol. **48:** 559–568, doi:10.1111/j.1529-8817.2012.01148.x

Houghton, J. T., and others. 2001. Climate change 2001: The scientific basis. Contribution of Working Group I to the 3rd assessment report of the Intergovernmental Panel on Climate Change. Cambridge Univ. Press.

Ihnken, S., S. Roberts, and J. Beardall. 2011. Differential responses of growth and photosynthesis in the marine diatom *Chaetoceros muelleri* to CO_2 and light availability. Phycologia **50:** 182–193, doi:10.2216/10-11.1

Kropuenske, L. R., and others. 2010. Strategies and rates of photoacclimation in two major Southern Ocean phytoplankton taxa: *Phaeocystis antarctica* (Haptophyta) and *Fragilariopsis cylindrus* (Bacillariophyceae). J. Phycol. **46:** 1138–1151, doi:10.1111/j.1529-8817.2010.00922.x

Martin, C. L., and P. D. Tortell. 2006. Bicarbonate transport and extracellular carbonic anhydrase activity in Bering Sea phytoplankton assemblages: Results from isotope disequilibrium experiments. Limnol. Oceanogr. **51:** 2111–2121, doi:10.4319/lo.2006.51.5.2111

Martin, J. H., R. M. Gordon, and S. E. Fitzwater. 1990. Iron in Antarctic waters. Nature **345:** 156–158, doi:10.1038/345156a0

McMinn, A., A. Pankowski, and T. Delfatti. 2005. Effect of hyperoxia on the growth and photosynthesis of Polar sea ice microalgae. J. Phycol. **41:** 732–741, doi:10.1111/j.1529-8817.2005.00095.x

Mehrbach, C., C. Culberson, J. Hawley, J., and R. Pytkovicz. 1973. Measurement of the apparent dissociation constants of carbonic acid in seawater at atmospheric pressure. Limnol. Oceanogr. **18:** 897–907, doi:10.4319/lo.1973.18.6.0897

Mitchell, C., and J. Beardall. 1996. Inorganic carbon uptake by an Antarctic sea-ice diatom, *Nitzschia frigida*. Polar Biol. **16:** 95–99, doi:10.1007/BF02390429

Moisan, T. A., and B. G. Mitchell. 1999. Photophysiological acclimation of *Phaeocystis antarctica* Karsten under light limitation. Limnol. Oceanogr. **44:** 247–258, doi:10.4319/lo.1999.44.2.0247

Neven, I. A., J. Stefels, S.M.A.C. van Heuven, H. J. W. de Baar, and J. T. M. Elzenga. 2011. High plasticity in inorganic carbon uptake by Southern Ocean phytoplankton in response to ambient CO_2. Deep-Sea Res. Part II **58:** 2636–2646, doi:10.1016/j.dsr2.2011.03.006

Palmqvist, K., J.-W. Yu, and M. R. Badger. 1994. Carbonic anhydrase activity and inorganic carbon fluxes in low- and high-Ci cells of *Chlamydomonas reinhardtii* and *Scenedesmus obliquus*. Physiol. Plant. **90:** 537–547, doi:10.1111/j.1399-3054.1994.tb08812.x

Pierrot, D. E., E. Lewis, and D. W. R. Wallace. 2006. MS Excel program developed for CO_2 system calculations. Carbon Dioxide Information Analysis Center, Oak Ridge National Laboratory, U.S. Department of Energy. Available from http://cdiac.ornl.gov/ftp/co2sys.

Raven, J. A., and W. J. Lucas. 1985. Energy costs of carbon acquisition, p. 305–324. *In* W. J. Lucas and J. A. Berry [eds.], Inorganic carbon uptake by aquatic photosynthetic organisms. American Society of Plant Physiologists.

Redfield, A. C. 1958. The biological control of chemical factors in the environment. Am. Sci. **46:** 205–222.

Riebesell, U., D. A. Wolf-Gladrow, and V. Smetacek. 1993. Carbon dioxide limitation of marine phytoplankton growth rates. Nature **361:** 249–251, doi:10.1038/361249a0

Rost, B., U. Riebesell, S. Burkhardt, and D. Sültemeyer. 2003. Carbon acquisition of bloom-forming marine phytoplankton. Limnol. Oceanogr. **48:** 55–67, doi:10.4319/lo.2003.48.1.0055

Sarmiento, J. L., and others. 2004. Response of ocean ecosystems to climate warming. Glob. Biogeochem. Cycles **18:** GB3003, doi:10.1029/2003GB002134

Silverman, D. N. 1982. Carbonic anhydrase. Oxygen-18 exchange catalyzed by an enzyme with rate contributing proton-transfer steps. Methods Enzymol. **87:** 732–752, doi:10.1016/S0076-6879(82)87037-7

Smetacek, V., P. Assmy, and J. Henjes. 2004. The role of grazing in structuring Southern Ocean pelagic ecosystems and biogeochemical cycles. Ant. Science **16:** 541–558, doi:10.1017/S0954102004002317

Thomson, P. G., A. McMinn, I. Kiessling, M. Watson, and P. M. Goldsworthy. 2006. Composition and succession of dinoflagellates and chrysophytes in the upper fast ice of Davis Station, East Antarctica. Polar Biol. **29:** 337–345, doi:10.1007/s00300-005-0060-y

Tilzer, M. M., B. von Bodungen, and V. Smetacek. 1985. Light-dependence of phytoplankton photosynthesis in the Antarctic Ocean: Implications for regulating productivity, p. 60–69. *In* W. R. Siegfried, P. R. Condy, and R. M. Laws [eds.], Antarctic nutrient cycles and food webs. Springer.

Tortell, P. D., C. L. Martin, and M. E. Corkum. 2006. Inorganic carbon uptake and intracellular assimilation by subarctic Pacific phytoplankton assemblages. Limnol. Oceanogr. **51:** 2102–2110, doi:10.4319/lo.2006.51.5.2102

———, C. D. Payne, C. Gueguen, R. F. Strzepek, P. W. Boyd, and B. Rost. 2008*a*. Inorganic carbon uptake by Southern Ocean phytoplankton. Limnol. Oceanogr. **53:** 1266–1278, doi:10.4319/lo.2008.53.4.1266

———, S. Trimborn, Y. Li, B. Rost, and C. D. Payne. 2010. Inorganic carbon uptake by Ross Sea phytoplankton across natural and experimental CO_2 gradients. J. Phycol. **46:** 433–443, doi:10.1111/j.1529-8817.2010.00839.x

———, and others. 2008*b*. The CO_2 sensitivity of Southern Ocean phytoplankton. Geophys. Res. Lett. **35:** L04605, doi:10.1029/2007GL032583

Trimborn, S., N. Lundholm, S. Thoms, K.-U. Richter, B. Krock, P. J. Hansen, and B. Rost. 2008. Inorganic carbon acquisition in potentially toxic and non-toxic diatoms: The effect of pH-induced changes in the seawater carbonate chemistry. Physiol. Plant. **133:** 92–105, doi:10.1111/j.1399-3054.2007.01038.x

———, D. Wolf-Gladrow, K.-U. Richter, and B. Rost. 2009. The effect of P_{CO_2} on the carbon acquisition and intracellular assimilation in four marine diatom species. J. Exp. Mar. Biol. Ecol. **376:** 26–36, doi:10.1016/j.jembe.2009.05.017

Wolf-Gladrow, D. A., and U. Riebesell. 1997. Diffusion and reaction in the vicinity of plankton: A refined model for inorganic carbon transport. Mar. Chem. **59:** 17–34, doi:10.1016/S0304-4203(97)00069-8

Yamasaki, Y., Y. Ohmichi, T. Shikata, M. Hirose, Y. Shimasaki, Y. Oshima, and T. Honjo. 2010. Species-specific allelopathic effects of the diatom *Skeletonema costatum*. Thalassas **27:** 21–32.

Associate editor: John Albert Raven

Received: 13 August 2012
Accepted: 10 December 2012
Amended: 13 December 2012